4D FWI with Reflection Oriented Workflow: Application to CO2 Monitoring at Sleipner Field

Fandy Adji Fachtony, Romain Brossier, Bastien Dupuy, Ludovic Métivier, Anouar Romdhane

4D FWI with Reflection Oriented Workflow: Application to CO_2 Monitoring at Sleipner Field

F. A. Fachtony[1], R. Brossier[1], B. Dupuy[3], L. Métivier[1,2] & A. Romdhane[4]

[1] Univ. Grenoble Alpes, ISTerre, F-38058 Grenoble, France
[2] CNRS, Univ. Grenoble Alpes, LJK, F-38058 Grenoble, France
[3] SINTEF Industry, Applied Geosciences Department, S.P. Andersens veg 15A, 7031 Trondheim, Norway
[4] Equinor, Trondheim, Norway

January 15, 2024

Main objectives CO_2 monitoring at Sleipner field with reflection oriented workflow 4D FWI.

New aspects covered

1. Application of the reflection oriented workflow for CO_2 monitoring on 3D Sleipner field data.

2. Application of the proposed workflow in full time lapse manner to the 3D Sleipner field data.

3 Estimation of the elastic properties of 3D sleipner field data in multi-parameter sense through JFWI.

Summary

Nowadays, the importance of carbon capture and storage (CCS) is rising due to the increase of attention on global climate changes. In industrial scale, Sleipner CCS facility is the first offshore storage operation and the longest operation in the world. For many years, Sleipner CO_2 injection site has been monitored by three dimensional seismic survey including a baseline survey prior to CO_2 injection. Several studies utilize full waveform inversion to estimate the CO_2 properties directly from seismic data. The common challenge on these FWI studies is offset limitation in the pre-2010 stramer data. Consequently, the diving waves cannot sample the deep part of the model. In our case study, we apply reflection oriented workflow which utilizes both diving waves and reflection waves through Joint Full Waveform Inversion (JFWI). In this sense, we can compensate the offset limitation of the data by utilizing the low wavenumber component of the reflected waves. In addition, we would like to tackle the monitoring problem in multi-parameter sense through JFWI as we can estimate the impedance and velocity properties during the workflow. In this sense, we can obtain both structural and quantitative properties based on impedance and velocity model obtained on single workflow.

4D FWI with Reflection Oriented Workflow: Application to CO_2 Monitoring at Sleipner Field

Introduction

Nowadays, the importance of carbon capture and storage (CCS) is rising. It is considered by the IPCC as an effective means to reduce the concentration of CO_2 in the atmosphere and mitigate the effects of the global climate changes. The Sleipner CCS facility has been the first offshore storage operation at industrial scale and the longest operated in the world. Since 1994 the Sleipner facility has been piloted and the first CO_2 injection into the Utsira formation started at 1996. Approximately, 1 million tons of CO_2 are being injected every year. For many years, Sleipner CO_2 injection site has been monitored by three dimensional seismic survey including a baseline survey prior to CO_2 injection.

Several studies utilize full waveform inversion (FWI) to estimate the CO_2 properties directly by minimizing the difference between observed and simulated seismic data (QueiBer and Singh, 2013; Romdhane and Querendez, 2014; Raknes et al., 2015). The common challenge on these FWI studies is the offset limitation in the available streamer data. Consequently, the diving waves cannot sample the deep part of the model. Therefore, FWI is limited to the reconstruction of high wavenumber perturbations (migration-like) at depth, which mainly contribute to the creation of interfaces rather than updating the velocity model. Additionally, previous studies are focused only on a single parameter estimation (velocity parameter). No other parameters, such as the impedance, are reconstructed, to further detail the CO_2 plume.

In our case study, we apply a reflection oriented workflow, which utilizes both diving and reflected waves through Joint Full Waveform Inversion (JFWI) (Zhou et al., 2015). This method helps up to compensate the offset limitation of the data by utilizing the transmitted energy between the reflectors and the receivers to constrain the low wavenumber component of the velocity along the reflection wavepath. This naturally brings us to consider the monitoring problem in a multi-parameter sense as JFWI, in the acoustic approximation, works with a parameterization separating the P-impedance and the P-wave velocity. We thus recover both structural and quantitative properties based on the impedance and velocity models obtained with a single workflow. This study is performed in the continuity of our previous work, where we analyzed on synthetic data the combination of the JFWI workflow with simultaneous time lapse strategy (Fachtony et al., 2023). In the current study, for the 4D aspect, we keep a simple parallel time-lapse strategy. The use of reflection oriented workflow with simultaneous time lapse strategy is expected in the future studies.

Joint Full Waveform Inversion (JFWI)

We recall here the JFWI formulation which makes use of a velocity-impedance $V_p - I_p$ parameterization. JFWI relies on a separation between early arrival (diving parts) and reflections (Zhou et al., 2015). The corresponding misfit function is

$$C_{JFWI}(V_P, I_P) = \frac{1}{2}\|W^{div}(d_{cal}(V_P, I_0) - d_{obs})\|^2_{L_2} + \frac{1}{2}\|W^{refl}(d_{cal}(V_P, I_P) - d^{obs})\|^2_{L_2}. \quad (1)$$

The first term measures the misfit between observed data d_{obs} and the calculated data $d_{cal}(V_P, I_0)$ in the smooth model (V_P, I_0) for the early arrivals, thanks to the weighing operator W^{div}. The second terms performs the same comparison for the reflection part thanks to the weighting operator W^{refl} with simulated data $d_{cal}(V_P, I_P)$ computed using a model with non-smooth reflectivity (V_P, I_P).

Following (Zhou et al., 2015), the gradient of C_{JFWI} with respect to V_P can be written as

$$\begin{aligned} \nabla_{V_P} C_{JFWI} &= u_0(V_P, I_0) \star \lambda_0^{div}(V_P, I_0) \ (\textit{banana-donuts}) \\ &+ \delta u(V_P, I_P) \star \lambda_0^{\mathrm{refl}}(V_P, I_0) + u_0(V_P, I_0) \star \delta\lambda^{\mathrm{refl}}(V_P, I_P) \ (\textit{rabbit ears}). \end{aligned} \quad (2)$$

The update on V_P is composed by the combination of tomographic diving waves and reflection wavepaths. $u_0(V_P, I_0)$ and $\lambda_0^{\mathrm{div}}(V_P, I_0)$ denote respectively the incident wavefield and the adjoint wavefield computed with the diving wave residuals as adjoint source, propagating in the smooth medium (V_P, I_0). $\delta u(V_P, I_P)$ is the scattering component of the incident wavefield due to the presence of I_P. $\lambda_0^{\mathrm{refl}}(V_P, I_0)$ denotes the

adjoint wavefield with the reflection data residuals as the adjoint source, computed inside the smooth medium (V_P, I_0). Finally $\delta\lambda^{\text{refl}}(V_P, I_P)$ is the scattering component of the adjoint wavefield due to the presence of I_P. The symbol $\star$ denotes the zero lag cross-correlation in time.

The gradient construction in (2) needs a reflectivity I_P which we compute through Impedance Waveform Inversion (IPWI). This consists in minimizing C_{JFWI} with respect to the impedance I_P. The gradient with respect to I_P can be written as

$$\nabla_I C_{\text{JFWI}} = u_0(V_P, I_P) \star \lambda_0^{\text{refl}}(V_P, I_P)\ (\textit{migration isochrones}). \tag{3}$$

Upon actual implementation, we rely on the reformulation in pseudo-time domain by Provenzano et al. (2022) to avoid repeated estimation of reflectivity/impedance information, which helps to mitigate velocity-depth ambiguity. In addition, we utilize a graph space optimal transport (GSOT) misfit function to mitigate potential cycle skipping issues (Métivier et al., 2019; **?**).

Application to the Sleipner field data

The Sleipner area is located at the west of Norway in the North Sea. It consists of the Sleipner West gas field and the Sleipner East condensate field. The CO_2 is stripped from Sleipner West field and injected to the Sleipner East field into the 200-300 m thick Utsira formation. The dataset consists of two 3D towed streamer survey from 1994 pre-injection as baseline data and 2008 post-injection as monitor data. Originally, the data set was acquired with 3000 m cable length and a recording length of 5.5 s for each shot. The air gun source was towed at 6 m depth with 18.75 m shooting interval. However, several processing steps have been applied to the data we have access to. They include: offset restriction to 1700 m, recording length reduction to 2.3 s, swell noise filtering, low cut filtering at 6.0 Hz, time-step resampling to 2.0 ms, and t^2 amplitude scaling for amplitude correction from 3D to 2D.

These conditions make the Sleipner field data challenging for FWI due to the limited offset and the absence of low frequency. To reduce the computational burden we decimate the data field by selecting one shot over five, with a total of 1002 shots for the baseline data and 1128 shots for the monitor data. We perform JFWI in a multiscale manner starting from 6-10 Hz up to 6-14 Hz with an intermediate 6-12 Hz band. The initial model is a 1D V_P model linearly increasing with depth. The initial density model is derived from this velocity model using a Gardner's relationship. To further decrease the computational cost, we also use a random subsampling strategy, with 128 sources per group of sources during the inversion. An average source wavelet is estimated by deconvolution in the frequency domain, focusing only on the diving waves part of the data.

We start the reflection oriented workflow by building the impedance through impedance waveform inversion (IPWI), windowing the short offset reflections up to 600 m of offset, and using an asymptotic preconditioner as in Provenzano et al. (2022). Two iterations are performed for each group of 128 sources, for a total of 12 iterations, so that each available shot gather is used at least once. The IPWI is performed on the baseline and monitor data in parallel. The results of IPWI on these datasets are supplied to JFWI as reflectivity information to construct the smooth V_P model. We run JFWI on full offsets up to 1.7 km with a linear depth preconditioning and 4 iterations per group of sources for a total of 24 iterations. Thanks to the pseudo-time domain formulation, the reflectors on I_P are updated in depth during JFWI simultaneously with V_P, which ensure the consistency of V_P and I_P at zero offset, therefore avoiding re-estimation for each velocity updates. However, we re-estimate the I_P every time we start with a new frequency band, as we perform the JFWI in multiscale manner. The V_P model obtained from the previous frequency band is used to estimate the I_P at the current frequency band, and we perform JFWI with the updated I_p.

Figure 1 illustrates the I_P model derived through impedance inversion. The CO_2 anomaly is observed to be distributed within the depth range of 700-1000 m. The depth slice at 800 m (Figure 1c) displays the plume's distribution spanning 2-4 km in the X direction and 1.5-3 km in the Y direction, which is expected. Furthermore, the 4D difference panel in Figure 2c reveals a distinct low V_P anomaly in the same region. From 1D profile in Figure 3, we can observe that the CO_2 anomalies are associated with 50 m/s velocity drop in the monitor model compared to the baseline model. To validate structural

consistency, we compare the I_P model obtained from JFWI at 14 Hz frequency with the publicly available migrated section (https://co2datashare.org/dataset/sleipner-4d-seismic-dataset) from full-band data in Figure 3. We can observe that the I_P model is able to predict the channel structure at a depth of 460 m (Figure 3a and 3b) and the CO_2 anomaly at 880 m (Figure 3c and 3d), which are consistent with the migrated section. For quality assessment, a data fit comparison between observed and calculated data based on V_P and I_P models from JFWI is presented in Figure 4, demonstrating a satisfactory fit for diving and reflected waves in both baseline and monitor data. Overall, JFWI exhibits promising outcomes within the current frequency band. Despite its relatively low frequency of 14 Hz, the reconstructed I_P model provides meaningful 3D structural information about CO_2, consistent with the full-band image. Additionally, both V_P and I_P models offer direct quantitative estimations of CO_2 properties. Compared to the prior studies of QueiBer and Singh (2013) and Romdhane and Querendez (2014) the V_P value of CO_2 is slightly overestimated, and the resolution of CO_2 thickness and distribution are lower. This overestimation is expected given the lower frequency (14 Hz) compared to the previous studies reaching up to 39 Hz, albeit in a 2D manner. Therefore, we expect to refine CO_2 parameter estimation by increasing the frequency band. It's worth noting that the JFWI method is typically employed for building an initial velocity model, therefore high resolution velocity model is not expected. To achieve a higher resolution velocity model, standard FWI can be performed using the JFWI model as a starting point in subsequent steps.

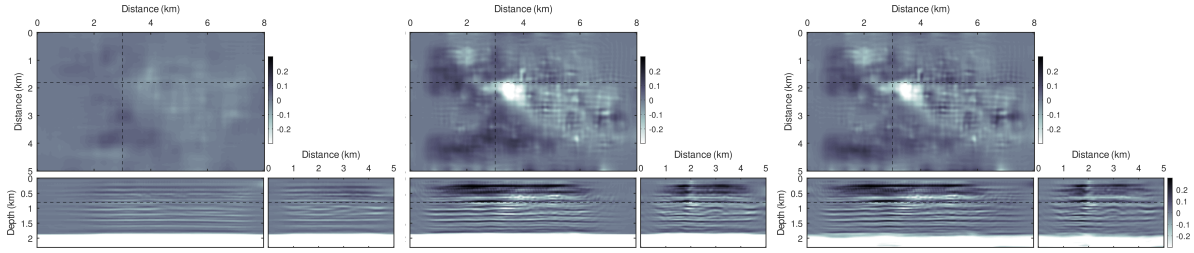

(a) (b) (c)

Figure 1 *Slices of the reconstructed impedance model at y=1.9 km, x=3.0 km and z=0.8 km. (a) reconstructed baseline, (b) reconstructed monitor, and (c) 4D difference between (a) and (b), CO_2 anomaly can be observed around 2-4 km in Y direction and 1.5-3 km in X direction ranging from 800-900 m.*

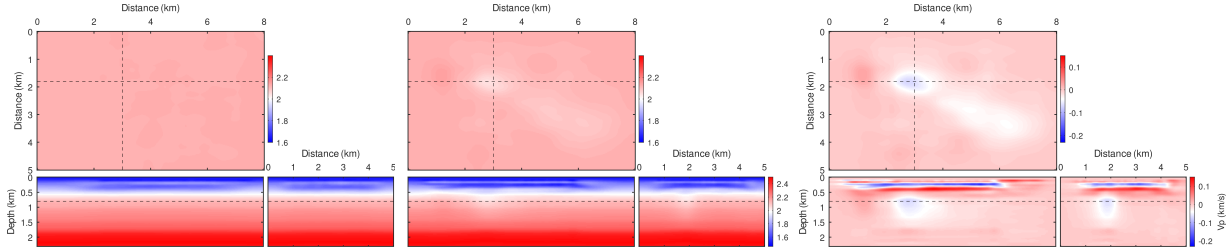

(a) (b) (c)

Figure 2 *Slices of the reconstructed velocity model at y=1.9 km, x=3.0 km and z=0.8 km. (a) reconstructed baseline, (b) reconstructed monitor, and (c) 4D difference between (a) and (b), CO_2 anomaly can be observed around 2-4 km in Y direction and 1.5-2.5 km in X direction ranging from 700-1000 m.*

Conclusions

We applied the reflection oriented workflow using JFWI to the Sleipner field data. We show that the reconstructed impedance and the velocity model from JFWI able to delineate the CO_2 anomaly quite well. Compared to the migrated section, structural information are consistent with the migrated section. For the quality check, the data fit shows that the obtained model from JFWI are able to fit both direct and reflection arrivals quite well with the observed data. Overall, this work contributes valuable insights into CO_2 distribution and quantitative properties, showcasing the potential of JFWI in CO_2 monitoring applications.

Acknowledgments

This study was partially funded by the SEISCOPE consortium (`http://seiscope2.osug.fr`), sponsored by AKER BP, CGG, DUG, EXXONMOBIL, GEOLINKS, JGI, PETROBRAS, SHELL, SINOPEC, TOTALENERGIES and by the NCCS consortium (`https://www.sintef.no/projectweb/nccs/`). This study was granted access to the HPC resources provided by the GRICAD infrastructure (https://gricad.univ-grenoble-alpes.fr), Cray Marketing Partner Network (`https://partners.cray.com`) and IDRIS/TGCC/CINES under the allocation 046091 made by GENCI.

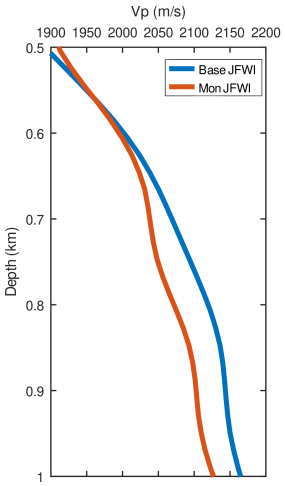

Figure 3 *Extracted 1D Velocity profile at y=1.9 km and x=3.0 km.*

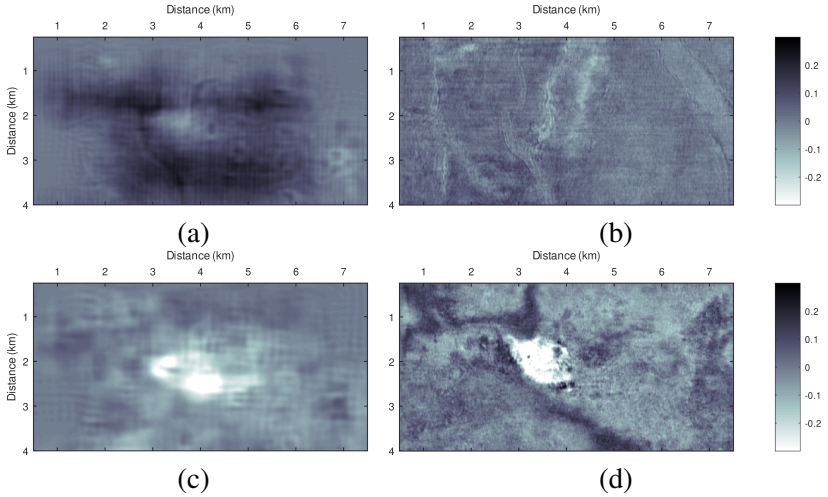

Figure 4 *Comparison between impedance model and migrated section. (a) impedance model at z=460 m, (b) migrated section at z=460 m, and (c) impedance model at z=880 m (d) migrated section z=880 m.*

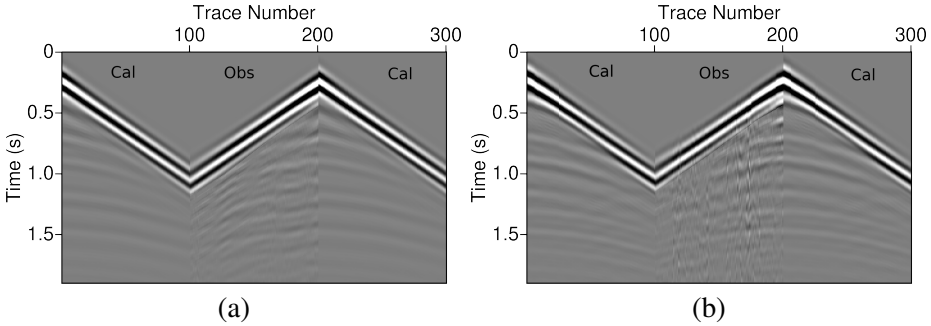

Figure 5 *Data fit between observed and calculated data. (a) baseline data fit, and (b) monitor data fit.*

References

Fachtony, F., Brossier, R., Dupuy, B., Métivier, L. and Romdhane, A. [2023] 4D FWI with Short Offset Data: a Reflection Oriented Approach. In: *84th Annual EAGE Meeting (Vienna)*, 2023. European Association of Geoscientists & Engineers.

Métivier, L., Brossier, R., Mérigot, Q. and Oudet, E. [2019] A graph space optimal transport distance as a generalization of L^p distances: application to a seismic imaging inverse problem. *Inverse Problems*, **35**(8), 085001.

Provenzano, G., Brossier, R. and Métivier, L. [2022] Robust and efficient waveform-based velocity-model-building by optimal-transport in the pseudotime domain: methodology. *Geophysics*, **in press**.

QueiBer, M. and Singh, S.C. [2013] Full waveform inversion in the time lapse mode applied to CO2 storage at Sleipner. *Geophysical Prospecting*, **61**(3), 537–555.

Raknes, E.B., Arntsen, B. and Weibull, W. [2015] Three-dimensional elastic full waveform inversion using seismic data from the Sleipner area. *Geophysical Journal International*, **202**(3), 1877–1894.

Romdhane, A. and Querendez, E. [2014] CO2 characterization at the Sleipner field with full waveform inversion: Application to synthetic and real data. *Energy procedia*, **63**, 4358–4365.

Zhou, W., Brossier, R., Operto, S. and Virieux, J. [2015] Full Waveform Inversion of Diving & Reflected Waves for Velocity Model Building with Impedance Inversion Based on Scale Separation. *Geophysical Journal International*, **202**(3), 1535–1554.